

Hans-Günther Döbereiner · Olaf Selchow
Reinhard Lipowsky

Spontaneous curvature of fluid vesicles induced by trans-bilayer sugar asymmetry

Received: 3 June 1998 / Revised version: 18 August 1998 / Accepted: 21 August 1998

Abstract We present measurements of the effective spontaneous curvature of fluid lipid bilayers as a function of trans-bilayer asymmetry. Experiments are performed on micrometer-scale vesicles in sugar solutions with varying species across the membrane. There are two effects leading to a preferred curvature of such a vesicle. The spontaneous curvatures of the two monolayers as well as their area difference combine into an effective spontaneous curvature of the membrane. Our technique for measuring this parameter allows us to use vesicle morphology as a probe for general membrane-solute interactions affecting elasticity.

Key words Vesicle shape · Spontaneous curvature · Bilayer couple · Sugar asymmetry

Introduction

The concept of interfacial elasticity (Helfrich 1973; Evans 1974; Safran 1998) has become an integral part in the theoretical description of fluid interfaces and biomembranes (Lipowsky 1992; Gompper and Schick 1994; Sackmann 1994; Seifert 1997). For instance, the shape of red blood cells (Deuling and Helfrich 1976; Mohandas and Evans 1994) and the morphology of fluid lipid vesicles (Berndl et al. 1990; Käs and Sackmann 1991; Farge and Devaux 1992; Döbereiner et al. 1997) is controlled by the elastic energy of the membrane and the cytoskeleton. Further, the steric interaction between fluctuating membranes (Helfrich 1978; Lipowsky and Leibler 1986) plays an important role in the stability of soft colloids.

The fundamental elastic constants which characterize a fluid membrane sheet are the bending elastic modulus and the spontaneous curvature (Helfrich 1973; Evans 1974). The bending modulus κ sets the energy scale. There is a

large literature on various techniques to measure this parameter (Seifert 1997). In contrast, the other parameter, the spontaneous curvature, has received considerably less attention by experimentalists. Introduced by Helfrich, it describes the preferred curvature of an unconstrained piece of membrane. In an early paper (Harbich et al. 1977), the spontaneous curvature of bilayer membranes was estimated from single snapshots of fluctuating vesicle shapes. The spontaneous curvature of mixed lipid monolayers was measured in a seminal work (Rand et al. 1990) via the osmotic force technique. They found the transition from lamellar to inverted hexagonal phases to be driven by a change in this parameter. The purpose of our work is to monitor for the first time the spontaneous curvature of fluid bilayers as a function of their aqueous environment. In this Letter, we constrain ourselves to an investigation of double-chain phospholipids. Under appropriate conditions, these molecules form closed bilayer capsules, i.e., vesicles, which are generally in mechanical but not in thermodynamic equilibrium due to the low solubility of these lipids in water. In addition, the flip-flop time between the monolayers is very slow. Thus, the area of each monolayer is conserved separately on experimentally relevant time scales. This is in contrast to the spontaneous vesicle formation observed with single chain surfactants (Kaler et al. 1992; Safran 1998). These amphiphilic systems are in thermodynamic equilibrium and may form a bulk vesicle phase.

For a phospholipid vesicle there are two different physical origins for bending in mechanical equilibrium (Svetina et al. 1985; Miao et al. 1994). First, the intrinsic spontaneous curvatures of the monolayers add up to a local spontaneous curvature of the membrane. Second, the difference in the number of molecules between two monolayers of a closed vesicle, i.e., the area difference between the inner and the outer monolayer, couples to the integrated mean curvature and gives rise to a non-local source of bending (Evans 1974; Helfrich 1974; Sheetz and Singer 1974). These two effects combine into an effective spontaneous curvature (Miao et al. 1994; Döbereiner et al. 1997). In this Letter, we present measurements of this

H.-G. Döbereiner (✉) · O. Selchow · R. Lipowsky
Max-Planck-Institut für Kolloid- und Grenzflächenforschung,
Kantstrasse 55, D-14513 Teltow-Seehof, Germany

quantity for unilamellar vesicles (10 μm) as a function of sugar asymmetry across the membrane. Indeed, we find two contributions to the effective spontaneous curvature corresponding to the monolayer and bilayer aspect of membrane architecture. This is accomplished by comparison of experimental mean vesicle shapes obtained via video phase-contrast microscopy with the theoretical shapes predicted by the area-difference-elasticity (ADE) model (Miao et al. 1994). The method is quite general and allows us to examine the spontaneous curvature induced by (almost) any kind of asymmetry across a membrane. To our knowledge, this is the first time such a study has been attempted. In the following, we recall briefly the main determinants of vesicle shape and describe the mapping of experimental shapes into the theoretical (shape) phase diagram.

Theoretical background

As shown recently (Döbereiner et al. 1997), experimental vesicle shapes are well described by the ADE model

$$H_{\text{ADE}} = \kappa \left(\frac{1}{2} \int dA (C_1 + C_2 - C_0)^2 + \frac{\alpha}{2} \frac{\pi}{AD^2} (\Delta A - \Delta A_0)^2 \right) \quad (1)$$

where the first term is the Helfrich bending energy with the modulus κ and the spontaneous curvature C_0 (Helfrich 1973). The second term gives the elastic contributions from the differential monolayer area ΔA , where the relative weight is determined by the ratio $\alpha = \tilde{\kappa}/\kappa$ of the two bending moduli (Raphael and Waugh 1996). The mean monolayer area and the thickness of the membrane are denoted by A and D , respectively. The relaxed area difference ΔA_0 describes the preferred curvature of the bilayer for $C_0 = 0$. In general, the proper dimensionless variable for preferred curvature (Döbereiner et al. 1997) is

$$\bar{c}_0 = c_0 + 2\pi\alpha(\Delta a_0 - \Delta a) \quad (2)$$

where $c_0 = C_0 R_A$, $\Delta a_0 = \Delta A_0 / 8\pi D R_A$, and Δa are reduced quantities scaled by $R_A = (A/4\pi)^{1/2}$. Vesicle shapes are obtained from minimizing Eq. (1) under the constraints of fixed area A and volume V (Miao et al. 1994). Thus, in addition to \bar{c}_0 , one needs to know the reduced volume $v = 3V/(4\pi R_A^3)$ to fully characterize a shape. We note that Eq. (2) captures the physics of the two sources of spontaneous curvature. Whereas c_0 is only a property of the vesicle membrane, the result of changing Δa_0 depends also on the reference shape via its integrated mean curvature which is proportional to Δa .

Experimental methods and data analysis

The mapping of an experimental mean vesicle shape into the (v, \bar{c}_0) parameter space has been described in detail

(Döbereiner et al. 1997). In this study, vesicle shapes were changed by controlling the sample temperature at a constant solution asymmetry across the membrane. Briefly, vesicles are stabilized by gravity at the bottom of the observation chamber in order to record long time sequences of fluctuating shapes. The usual rotational symmetry is slightly broken and prolate vesicles appear more circular in the plane including their long axis. This introduces a new dimensionless variable (Kraus et al. 1995), $g \equiv g_0 \Delta\rho R_A^4/\kappa$, measuring the relative importance of gravity, where g_0 is the local acceleration and $\Delta\rho$ is the excess mass density of the interior solution. The chamber floor is modeled by a soft repulsive substrate potential (Döbereiner et al. 1997). As we shall see later, such an assumption is slightly inconsistent. Effects of adhesion to the substrate should be included in a full data analysis. However, in our case the vesicles adhere at most weakly and we will ignore adhesion in a first approximation. Theoretical vesicle shapes are obtained via direct energy minimization for a given gravity strength g and compared to the experimental shapes. In this way, one obtains a one-to-one mapping of experimental shapes characterized by appropriate mean Fourier amplitudes of their contours (see below) into the (v, \bar{c}_0) parameter space. Thus, the effective spontaneous curvature \bar{c}_0 can be measured for a particular vesicle under observation. Due to the relatively small shape changes, the error in determining \bar{c}_0 is only slightly smaller than one in dimensionless units. Near the first-order budding transition, where a small satellite is expelled from the parent vesicle, the error is intrinsically larger due to the finite lifetime of the metastable prolate vesicle (Döbereiner et al. 1995). Although our measurement of the spontaneous curvature requires theoretical input, we note that the procedure is, indeed, only weakly model dependent. Since vesicle shapes do not depend on the ratio α of the elastic moduli, the precise value of this parameter is irrelevant for a measurement of the combined quantity; see Eq. (2). Apart from corrections due to gravity, the only assumption is that vesicles assume the shape of lowest mechanical bending energy of their membrane subject to constraints on area and volume. This has clearly been shown to be true in quite a number of studies (Käs and Sackmann 1991; Farge and Devaux 1992; Mui et al. 1995; Döbereiner et al. 1997).

We have constructed a micro-chamber, where the outer solution can be exchanged during observation of a vesicle. This chamber basically consists of a Teflon spacer sealed by a sapphire window on top and a common cover-slide on the bottom. Sapphire was used for the top window because of its high thermal conductivity, guaranteeing optimal thermal contact to a thermostat water cushion. Solution exchange is realized via two tubing ports connecting the chamber to a microliter pump and a liquid reservoir. Porous walls in the inlet path homogenize the flow. Pumping with typical rates of about 1 $\mu\text{l/s}$ results in an almost homogeneous shear flow at the vesicle position with a shear rate on the order of 1 s^{-1} . We have observed that (1) shear flow lifts the vesicles from the chamber bottom where they have accumulated due to gravity and (2) even minute shear flow has considerable influence on the vesicle shapes. Sta-

tionary non-equilibrium shapes are generally quite different from the corresponding equilibrium shapes. Indeed, we have seen oblate vesicles being deformed into prolates under shear flow. The first finding points to an effective hydrodynamic repulsion of the vesicles from the wall. As it is clear from the above remarks, equilibrium shape analysis was done only after the solution had been exchanged and fluid flow had come to a complete stop.

The described chamber-thermostat combination is mounted on the object table of an inverted microscope equipped with a CCD camera which directly passes the phase-contrast images of the vesicles to the video-board of a Unix workstation. There, the relevant shape parameters are extracted in real time (25 fps) via Fourier analysis of the vesicle contours. A half-contour may be written in terms of its arclength s which starts at the north pole ($s = 0$) and ends at the south pole ($s = s^*$). A representation which will be convenient for our purposes is

$$\psi(s) = \pi \frac{s}{s^*} + \sum_{n=1}^{\infty} a_n \sin\left(n \pi \frac{s}{s^*}\right) \quad (3)$$

where $\psi(s)$ is the angle between the polar axis and the outward-pointing normal to the curve. For prolate vesicles, the amplitude a_2 is a measure of ellipticity, whereas a_3 describes a pear-shape-like symmetry breaking. The spontaneous curvature of the vesicles is essentially encoded in the amplitude a_4 (Döbereiner et al. 1997). In Fig. 1, an experimental example of the probability distribution of the amplitude (a_2, a_4) is shown.

Vesicles are swollen from stearyl-oleoyl-phosphocholine (SOPC) and dimyristoyl-phosphocholine (DMPC) in 75 mosmol raffinose solution and incubated in an iso-

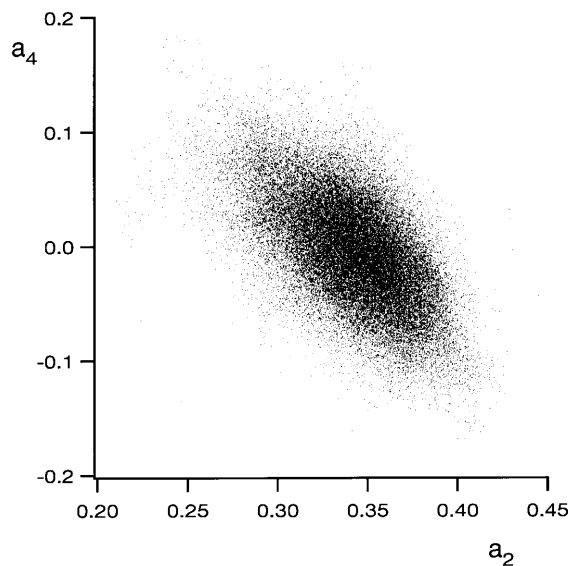


Fig. 1 Experimental distribution of the contour amplitudes (a_2, a_4). Their mean values uniquely fix the theoretical shape parameters (ν, \bar{c}_0). The plot contains over 53000 points corresponding to more than 35 min of real time data recorded at a rate of 25 video frames per second

osmolal raffinose-glucose solution (9:1). Depending on their radius, the vesicles experience a varying buoyance force and the larger ones accumulate quickly on the bottom of the chamber. Suitable prolate vesicles are selected for analysis and observed under the microscope. The concentration of glucose in the outer solution is then gradually increased at iso-osmolal conditions, $N_{ra}^{in} = N_{gl}^{ex} + N_{ra}^{ex}$, and the mean shape determined for several different sugar ratios $x = N_{gl}^{ex}/(N_{gl}^{ex} + N_{ra}^{ex})$. Due to the low permeability of the membrane to sugar molecules, the solution in the interior of the vesicles stays constant on experimentally relevant time scales. This has been confirmed by monitoring the optical contrast across the membrane due to sugar asymmetry.

This protocol creates an increasing solution asymmetry across the vesicle membrane. The density difference between the inner and outer solution increases with increasing asymmetry. Combining measurements of osmolality with densitometry, we get an almost linear relationship, $\Delta\rho \approx x \cdot 10 \text{ g/l}$, at 75 mosmol. Thus, for a fixed vesicle radius, the gravitational parameter g is linearly increasing with x .

Results and discussion

Prolate vesicles are expected to be pressed against the bottom of the chamber by gravity and become progressively flattened with increasing g . Indeed, for fixed spontaneous curvature, theory predicts a gravity-induced prolate-oblate transition (Kraus et al. 1995). However, the experimental finding is that the vesicles usually become more elongated when increasing the density difference between the interior and the exterior of the vesicle by raising the external glucose concentration. We conclude that the spontaneous curvature of the vesicles is in fact not constant but gets larger and counteracts the rising gravitational force. Indeed, the fluctuation spectra acquire the characteristics of spinodal fluctuations near the budding instability (Döbereiner et al. 1995), i.e., there is a strong increase in the a_3 fluctuations with increasing asymmetry. For vesicles which were sufficiently close to the prolate-oblate transition, i.e., those exhibiting large a_2 fluctuations (Döbereiner and Seifert 1996), we found a shift of the maximum of the fluctuation spectrum from $n = 2$ to $n = 3$. In some cases, we could even induce budding. Thus, one cannot evade the conclusion – even without any detailed analysis – that the effective spontaneous curvature of the membrane must have increased. One can also decrease spontaneous curvature by decreasing sugar asymmetry across the membrane. In that way, one vesicle which was found to be oblate at high glucose concentration was driven across the stomatocyte phase boundary (Seifert 1997) to exhibit an inward budded morphology. We also observe a slight decrease of the reduced volume ν when increasing sugar asymmetry x at iso-osmolal conditions. This apparent change of ν could be due to a weak adhesion of the vesicles to the substrate, which we did not include in our analysis.

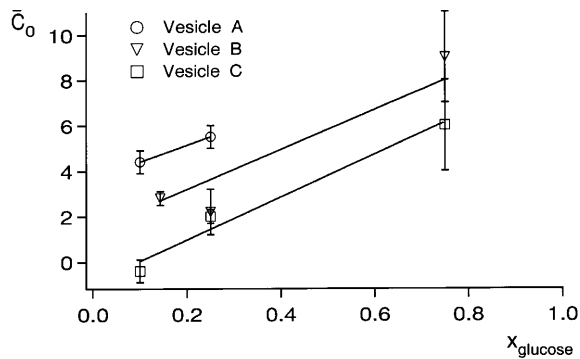


Fig. 2 Effective spontaneous curvature \bar{c}_0 as a function of sugar asymmetry x across the membrane in 75 mosmol raffinose-glucose solution. Vesicles contain pure raffinose solution. The percentage of glucose on the outside is given by x

The qualitative effects just described are quantified in Fig. 2, where the effective spontaneous curvature \bar{c}_0 of three different vesicles is displayed as a function of the glucose content x of the exterior solution. Individual linear fits to the data give a universal slope with different offsets in \bar{c}_0 at $x = 0$ for each vesicle. Thus, even for a symmetric solution across the membrane there is some asymmetry of the membrane left. We attribute this to a variation in Δa_0 between the different vesicles. For nanometer-scale vesicles, it has already been shown by driven lipid flip-flop that changes in the equilibrium area difference Δa_0 result in a corresponding change in vesicle morphology (Mui et al. 1995). It became also apparent in tether pulling experiments (Waugh et al. 1992; Yeung 1994) that the monolayer area difference contributes considerably to membrane curvature. Variations in Δa_0 explain why one usually finds quite a zoo of vesicle shapes even in symmetric buffer solutions. We note that it is therefore not generally correct to set the (effective) spontaneous curvature of a vesicle to zero, as it is often done in the literature. Since $\Delta a_0 \approx \Delta N \bar{a}_{\text{mol}}$ is essentially determined by the difference in the number of molecules ΔN , it is clear that the vesicles will have a distribution in Δa_0 fixed at the time of membrane closure. Thus, this quantity is dependent on the sample preparation and the particular history of the vesicle under investigation. In contrast, the common slope of the data in Fig. 2 points to an intrinsic interaction of the sugar molecules with the membrane. We find $\bar{c}_0 \approx (9.5 \pm 1.5) x$. Within experimental resolution, there is no difference between SOPC and DMPC detectable. We note that to leading order, one expects a linear dependence of \bar{c}_0 on sugar asymmetry x from symmetry considerations. The limited number of data points do not permit us to detect any deviation from linearity. However, the fact that individual linear fits give a universal slope allows us to extract the numerical value of this slope with some confidence.

From the theoretical point of view, the sugar molecules may be viewed as small particles which interact with the membrane surfaces but are essentially insoluble in the interior of the lipid bilayer. If the interaction between the sugar molecules and the membrane surfaces is repulsive,

two different sugar species induce a spontaneous curvature provided these two species differ in their size. Indeed, the two depletion layers in front of the membrane then differ in their thickness and the two species suffer a different loss of translational entropy. In order to minimize this entropy loss, the membrane has a tendency to curve toward the larger particles. Since glucose is smaller than raffinose, this entropic mechanism curves the membrane away from the glucose molecules, as observed in our experiments.

In the simplest approximation, one considers a dilute solution of quasi-spherical raffinose and glucose particles which have the characteristic size R_{ra} and R_{gl} , respectively. For a bilayer membrane with thickness l_{me} at temperature T , one then finds the spontaneous curvature (Lipowsky and Döbereiner 1998)

$$c_0 = (kT/2 \kappa) R_A (R_{\text{ra}} - R_{\text{gl}}) [l_{\text{me}} + R_{\text{ra}} + R_{\text{gl}}] n x \quad (4)$$

where $n \equiv N_{\text{ra}}^{\text{in}}/V$ is the sugar concentration of the solution. A rough estimate of the molecular dimensions leads to $R_{\text{ra}} \approx 0.8$ nm and $R_{\text{gl}} \approx 0.6$ nm, whereas the vesicle membrane is characterized by $R_A \approx 10$ μm and $l_{\text{me}} \approx 4$ nm. The studied sugar osmolality of 75 mosmol corresponds to a sugar concentration $n \approx 1/20$ nm³. If one inserts these values into Eq. (4), one obtains $c_0 \approx 11$, which must be compared with the data shown in Fig. 2 which give $c_0 \approx 10 x$. Thus, this rather simple picture leads to an estimate of c_0 which has the correct order of magnitude.

Experimental data which were obtained for the uptake of glucose by vesicle dispersions seem to indicate that glucose is adsorbed onto phospholipid membranes (Bummer and Zografis 1988). We are not aware of corresponding data for raffinose. Since the attractive interactions can arise from several hydrogen bonds, it is not obvious how this interaction differs for different sugar species.

Theoretically, it follows from the Gibbs adsorption equation that relatively small particles which are adsorbed onto the membrane surface reduce the interfacial tension of this surface. Thus, if glucose is adsorbed only onto the exterior membrane surface, the membrane should curve away from the exterior solution, as observed. The magnitude of the corresponding contribution to the spontaneous curvature can be calculated in the framework of a simple Langmuir-type model for monolayer adsorption. One then finds (Lipowsky and Döbereiner 1998) that

$$c_0 = (kT/2 \kappa) R_A (l_{\text{me}} + 2R_{\text{gl}}) \Gamma_{\text{gl}} \quad (5)$$

where Γ_{gl} is the glucose coverage, i.e., the number of adsorbed glucose molecules per unit area. The data by Bummer and Zografis (1988) imply that Γ_{gl} increases roughly linearly with increasing bulk concentration n_{gl} as $\Gamma_{\text{gl}} \approx B n_{\text{gl}}$ with $B \approx 3 \times 10^{15}$ m/mol. It then follows from Eq. (5) that $c_0 \approx 260 x$ for the parameter values as used before. Compared to our experimental data, this is too large by one order of magnitude. Thus, if we accept the results of Bummer and Zografis, our data seem to imply that raffinose is also adsorbed onto the membrane surfaces but that this adsorption is not as strong as for glucose. Indeed, the two contributions arising from the adsorption of glucose and of raffinose would compensate each other to some extent,

and the bilayer would curve away from the more strongly adsorbed particles.

In summary, both depletion and adsorption could be responsible for the observed increase in the spontaneous curvature with increasing glucose concentration. In order to discriminate between the two possibilities, one has to determine the concentration profiles of the sugar molecules in front of the lipid membranes. This can be done, for example, by performing ellipsometry with lipid monolayers at the air-water interface.

The technique described above for measuring the effective spontaneous curvature is quite general and can be applied to a large number of systems. Vesicle shapes may serve as a morphological probe for the investigation of general interfacial interactions affecting the elastic properties of membranes. Two specific examples, which have attracted considerable theoretical interest, are electrolytes (Winterhalter and Helfrich 1988, 1992; Mitchell and Ninham 1989) and polymers (Lipowsky 1995; Eisenriegler et al. 1996; Hiergeist and Lipowsky 1996) interacting with (charged) membranes. We conclude by remarking that the sensitivity of the membrane shape to minute differences in total area between the two monolayers allows for in situ characterization of enzyme, e.g., phospholipase, activity (Wick et al. 1996), and provides a non-invasive technique for studying lipid flip-flop (Mui et al. 1995).

Acknowledgements We thank W. Fenzl, G. Gompper, C. Hiergeist, M. Kraus, E. Sackmann, U. Seifert, and M. Wortis for useful discussions. Special thanks to M. Kraus for supplying us with numerical data and the code to perform shape calculations including gravity.

References

- Berndl K, Käs J, Lipowsky R, Sackmann E, Seifert U (1990) Shape transformations of giant vesicles: extreme sensitivity to bilayer asymmetry. *Europhys Lett* 13: 659–664
- Bummer PM, Zografi G (1988) The association of D-glucose with unilamellar phospholipid vesicles. *Biophys Chem* 30: 173–183
- Deuling HJ, Helfrich W (1976) Red blood cell shapes as explained on the basis of curvature elasticity. *Biophys J* 16: 861–868
- Döbereiner H-G, Seifert U (1996) Giant vesicles at the prolate-oblate transition: a macroscopic bistable system. *Europhys Lett* 36: 325–330
- Döbereiner H-G, Evans E, Seifert U, Wortis M (1995) Spinodal fluctuations of budding vesicles. *Phys Rev Lett* 75: 3360–3363
- Döbereiner H-G, Evans E, Kraus M, Seifert U, Wortis M (1997) Mapping vesicle shapes into the phase diagram: a comparison of experiment and theory. *Phys Rev E* 55: 4458–4474
- Eisenriegler E, Hanke A, Dietrich S (1996) Polymers interacting with spherical and rod-like particles. *Phys Rev E* 54: 1134–1152
- Evans E (1974) Bending resistance and chemically induced moments in membrane bilayers. *Biophys J* 14: 923–931
- Farge F, Devaux P (1992) Shape changes of giant liposomes induced by an asymmetric transmembrane distribution of phospholipids. *Biophys J* 61: 347–357
- Gompper G, Schick M (1994) In: Domb C, Lebowitz JL (eds) *Phase transitions and critical phenomena*, vol 16. Academic Press, San Diego
- Harbich W, Deuling HJ, Helfrich W (1977) Optical observation of rotationally symmetric lecithin vesicle shapes. *J Phys* 38: 727–729
- Helfrich W (1973) Elastic properties of lipid bilayers: theory and possible experiments. *Z Naturforsch* 28c: 693–703
- Helfrich W (1974) Blocked lipid exchanges in bilayers and its possible influence on the shape of vesicles. *Z Naturforsch* 29: 510–515
- Helfrich W (1978) Steric interaction of fluid membranes in multilayer systems. *Z Naturforsch* 33: 305–315
- Hiergeist C, Lipowsky R (1996) Elastic properties of polymer-decorated membranes. *J Phys II* 6: 1465–1481
- Kaler EW, Herrington KL, Zasadzinski JAN (1992) Spontaneous vesicles and other solution structures in catanionic mixtures. *Mater Res Soc Symp Proc* 248: 3–9
- Käs J, Sackmann E (1991) Shape transitions and shape stability of giant phospholipid vesicles in pure water induced by area-to-volume changes. *Biophys J* 60: 825–844
- Kraus M, Seifert U, Lipowsky R (1995) Gravity-induced shape transformations of vesicles. *Europhys Lett* 32: 431–436
- Lipowsky R (1992) The conformation of membranes. *Nature* 349: 475–481
- Lipowsky R (1995) Bending of membranes by anchored polymers. *Europhys Lett* 30: 197–202
- Lipowsky R, Döbereiner H-G (1998) Vesicles in contact with nanoparticles and colloids. *Europhys Lett* 42: 219–225
- Lipowsky R, Leibler S (1986) Unbinding transitions of interacting membranes. *Phys Rev Lett* 56: 2541–2544
- Miao L, Seifert U, Wortis M, Döbereiner H-G (1994) Budding transitions of fluid-bilayer vesicles: the effect of area-difference elasticity. *Phys Rev E* 49: 5389–5407
- Mitchell DJ, Ninham BW (1989) Curvature elasticity of charged membranes. *Langmuir* 5: 1121–1123
- Mohandas N, Evans EA (1994) Mechanical properties of the red cell membrane in relation to molecular structure and genetic defects. *Annu Rev Biophys Biomol Struct* 23: 787–818
- Mui BL-S, Döbereiner H-G, Madden TD, Cullis PR (1995) Influence of trans-bilayer area asymmetry on the morphology of large unilamellar vesicles. *Biophys J* 69: 930–941
- Rand RP, Fuller NL, Gruner SM, Parsegian VA (1990) Membrane curvature, lipid segregation, and structural transitions for phospholipids under dual-solvent stress. *Biochemistry* 29: 76–87
- Raphael RM, Waugh R (1996) Accelerated interleaflet transport of phosphatidylcholine molecules in membranes under deformation. *Biophys J* 71: 1374–1388
- Sackmann E (1994) Membrane bending energy concept of vesicle and cell-shapes and shape transitions. *FEBS Lett* 346: 3–16
- Safran SA (1998) Curvature elasticity of thin films. *Adv Phys* (in press)
- Seifert U (1997) Configurations of fluid membranes and vesicles. *Adv Phys* 46: 13–137
- Sheetz MP, Singer SJ (1974) Biological membranes as bilayer couples. A molecular mechanism of drug-erythrocyte interactions. *Proc Natl Acad Sci USA* 71: 4457–4461
- Svetina S, Brumen M, Žekš B (1985) Lipid bilayer elasticity and the bilayer couple interpretation of red cell shape transformations and lysis. *Stud Biophys* 110: 177–184
- Waugh RE, Song J, Svetina S, Žekš B (1992) Local and nonlocal curvature elasticity in bilayer membranes by tether formation from lecithin vesicles. *Biophys J* 61: 974–982
- Wick R, Angelova MI, Walde P, Luisi PL (1996) Microinjection into giant vesicles and light microscopy investigation of enzyme-mediated vesicle transformations. *Chem Biol* 3: 105–111
- Winterhalter M, Helfrich H (1988) Effect of surface charge on the curvature elasticity of membranes. *J Phys Chem* 92: 6865–6867
- Winterhalter M, Helfrich H (1992) Bending elasticity of electrically charged bilayers: coupled monolayers, neutral surfaces, and balancing stresses. *J Phys Chem* 96: 327–330
- Yeung T (1994) Mechanism of inter-monolayer coupling in fluid surfactant bilayers. PhD Thesis, University of British Columbia, Vancouver, B.C., Canada